

## Supporting Information

### **Amino-functionalized SiC electrodes for highly sensitive simultaneous detection of Pb<sup>2+</sup>, Cd<sup>2+</sup>, Cu<sup>2+</sup>, Hg<sup>2+</sup>**

Xin Wang<sup>1</sup>, Linlin Zhou<sup>1,2\*</sup>, Xinmei Hou<sup>1,3\*</sup>

<sup>1</sup>. *Institute for Carbon Neutrality, Beijing Advanced Innovation Center for Materials Genome Engineering, University of Science and Technology Beijing, Beijing 100083, China*

<sup>2</sup>. *School of Materials, Shenzhen Campus of Sun Yat-sen University, Shenzhen 518107, China*

<sup>3</sup>. *Institute of Steel Sustainable Technology, Liaoning Academy of Materials, Shenyang 110000, China*

\* Author to whom correspondence should be addressed e-mails:

[zhoulin7@mail.sysu.edu.cn](mailto:zhoulin7@mail.sysu.edu.cn) (L. L. Zhou)

[houxinmeiustb@ustb.edu.cn](mailto:houxinmeiustb@ustb.edu.cn) (X. M. Hou)

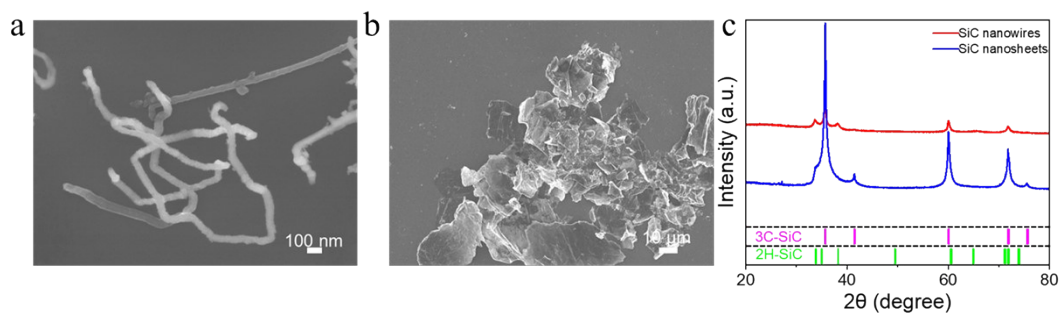


**Fig. S1** SEM images of (a) SiC nanowires (b) SiC nanosheets (c) XRD patterns of SiC nanowires and nanosheets

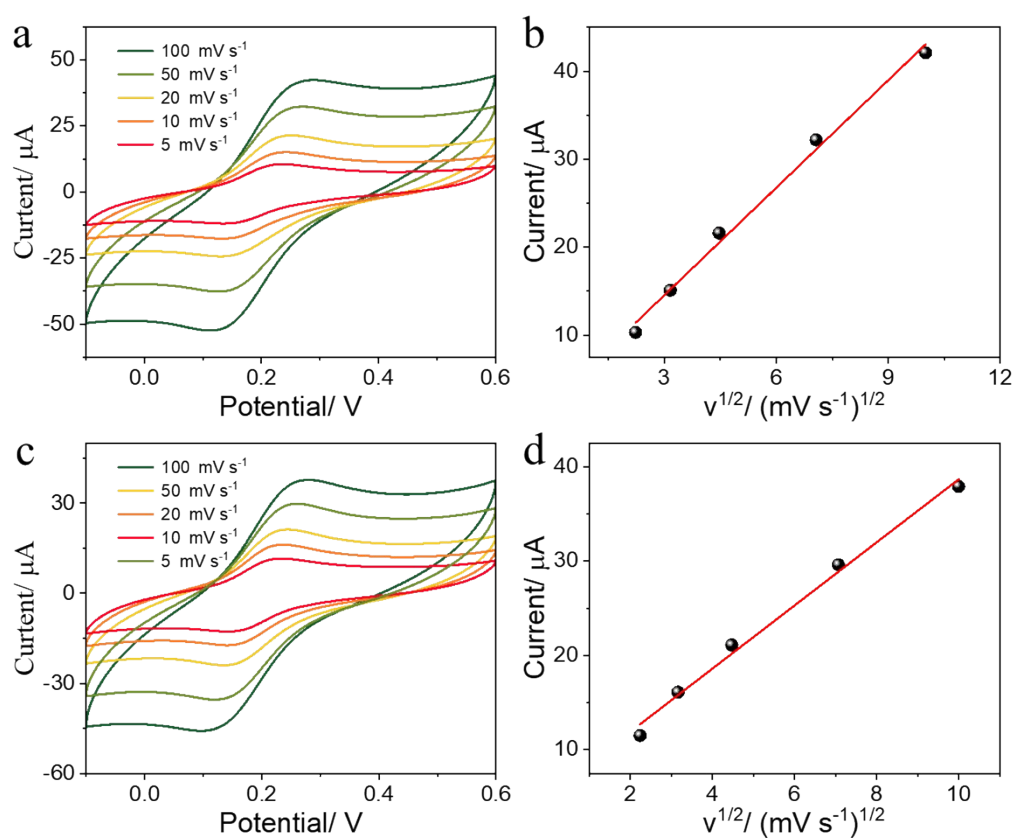


**Fig. S2** (a, c) CV curves recorded at different scan rates (5, 10, 20, 50, and 100 mV s<sup>-1</sup>) in 0.1 M KCl containing 0.5 mM K<sub>3</sub>[Fe(CN)<sub>6</sub>]. (b, d) corresponding linear plots of anodic peak current (I<sub>p</sub>) versus the square root of scan rate (v<sup>1/2</sup>) at (a, b) NH<sub>2</sub>-SiC nanosheet modified electrode and (c, d) NH<sub>2</sub>-SiC nanowire modified electrode.

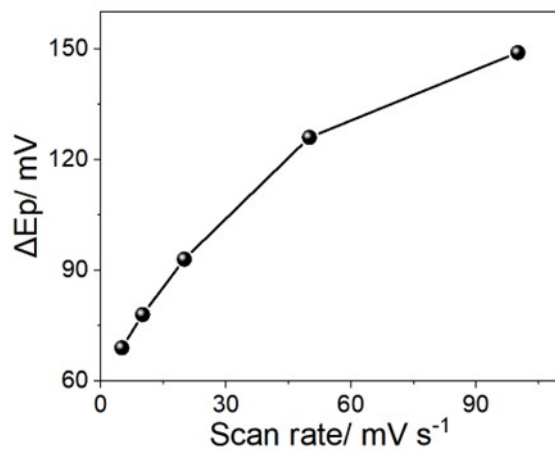


**Fig. S3** Dependence of the peak-to-peak separation ( $\Delta E_p$ ) on scan rate for the  $[\text{Fe}(\text{CN})_6]^{3-/4-}$  redox couple at the modified electrode in 0.1 M KCl containing 0.5 mM  $\text{K}_3[\text{Fe}(\text{CN})_6]$ .

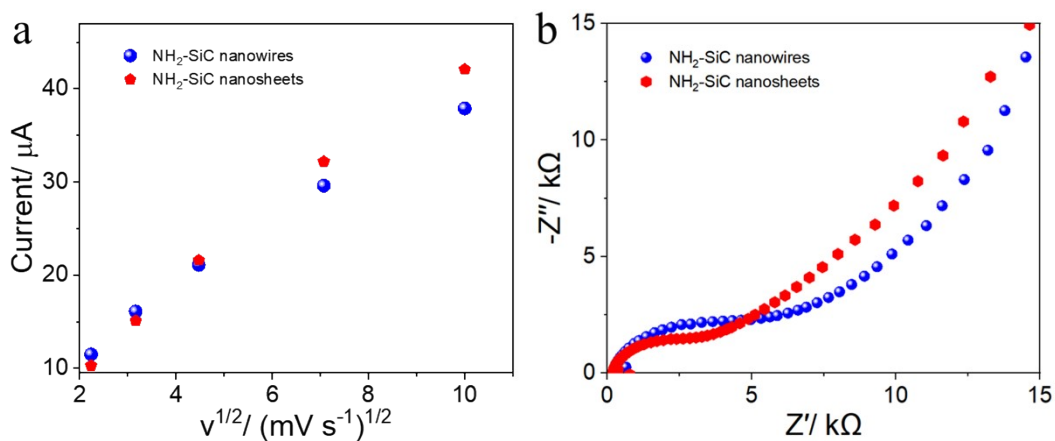


**Fig. S4** a)  $I_p$  vs.  $v^{1/2}$  plots and (b) Nyquist plots of  $\text{NH}_2\text{-SiC}$  nanowires and nanosheets modified GCE electrodes.

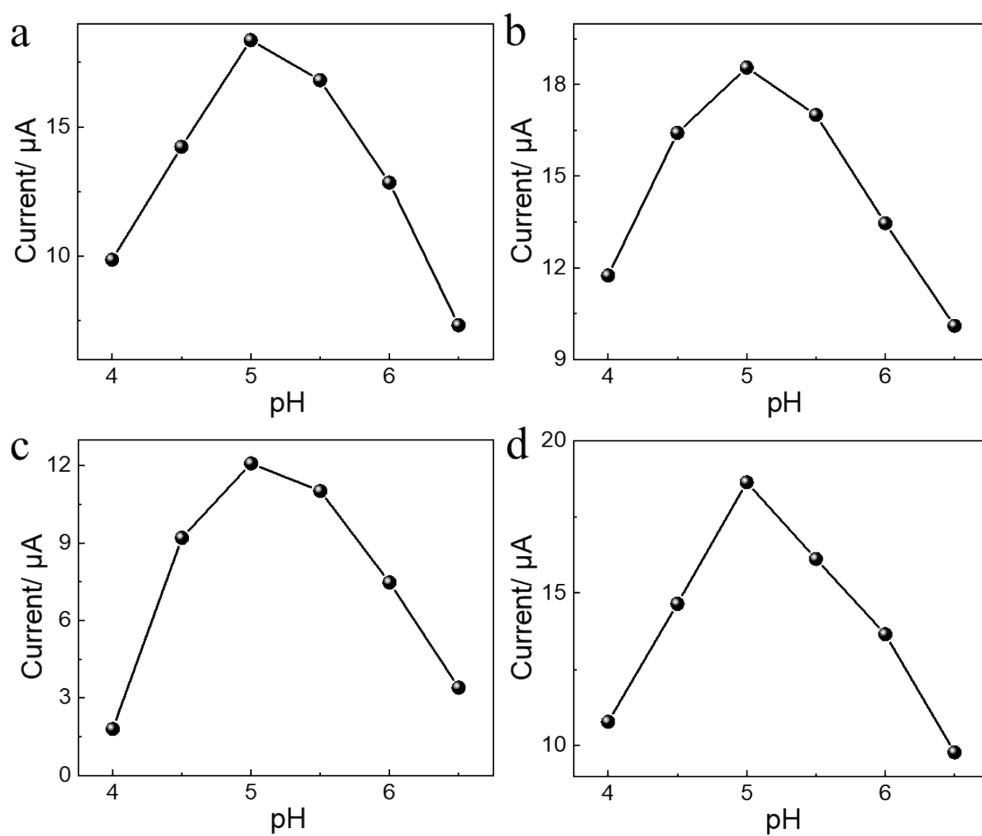


**Fig. S5** Optimum pH conditions for  $\text{NH}_2\text{-SiC}$  nanowires-modified electrodes toward (a)  $\text{Cd}^{2+}$  (b)  $\text{Pb}^{2+}$  (c)  $\text{Cu}^{2+}$  (d)  $\text{Hg}^{2+}$

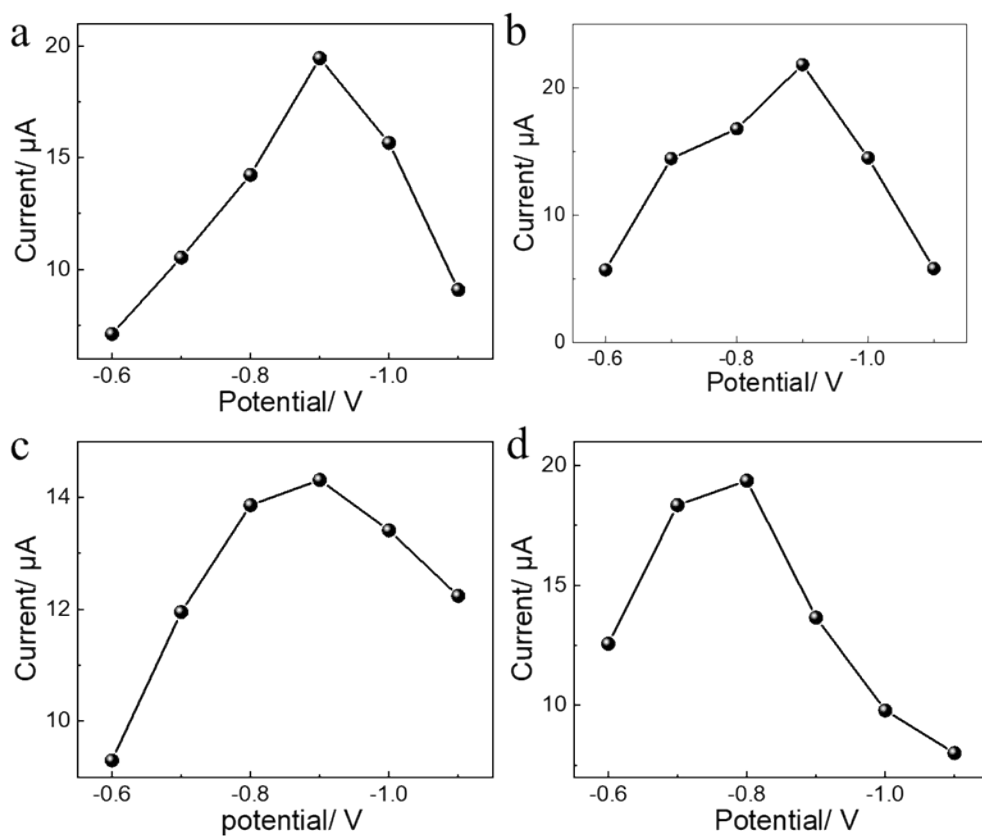


**Fig. S6** Optimum deposition potential conditions for  $\text{NH}_2\text{-SiC}$  nanowires-modified electrodes toward (a)  $\text{Cd}^{2+}$  (b)  $\text{Pb}^{2+}$  (c)  $\text{Cu}^{2+}$  (d)  $\text{Hg}^{2+}$

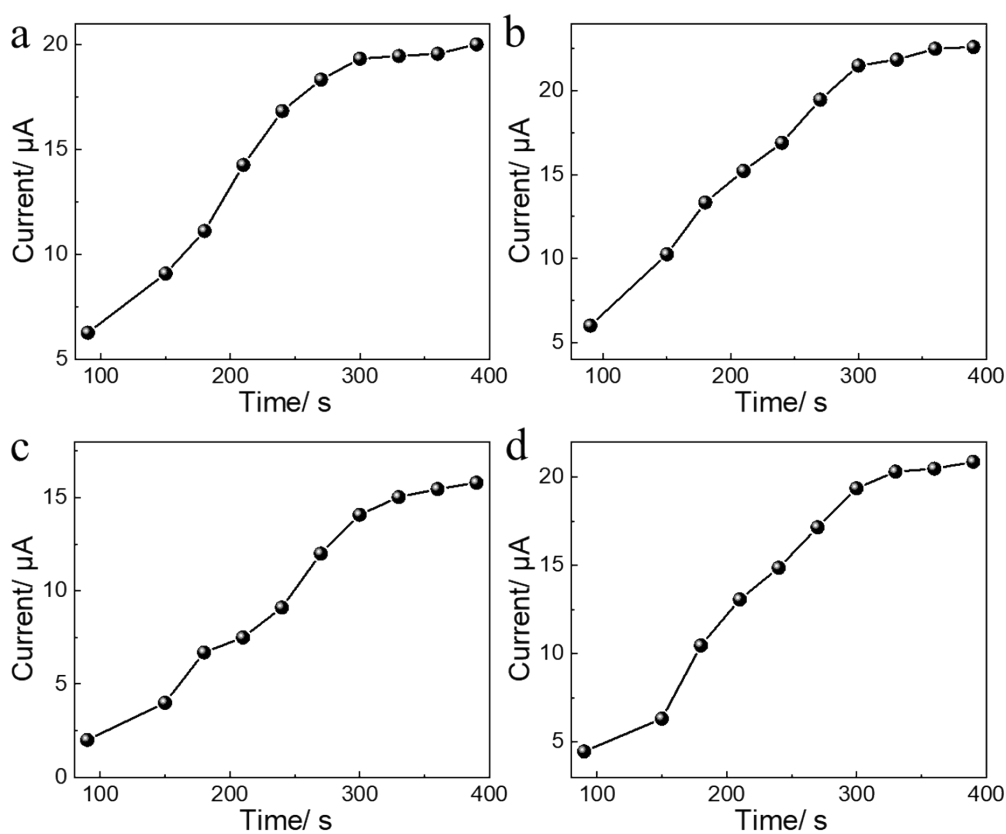


**Fig. S7** Optimum deposition time conditions for  $\text{NH}_2\text{-SiC}$  nanowires-modified electrodes toward (a)  $\text{Cd}^{2+}$  (b)  $\text{Pb}^{2+}$  (c)  $\text{Cu}^{2+}$  (d)  $\text{Hg}^{2+}$

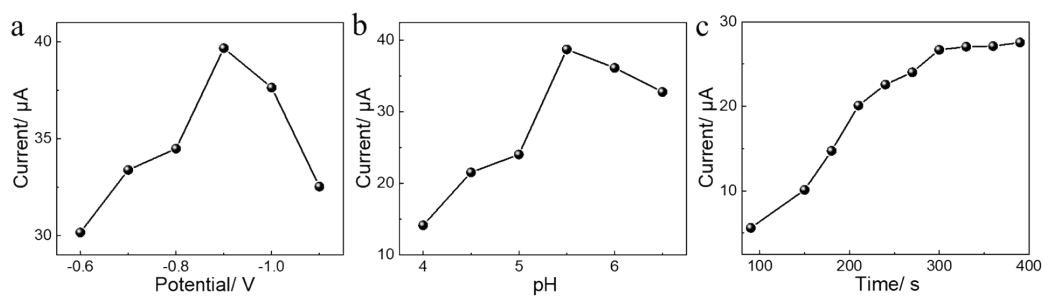


**Fig. S8** Optimum experimental conditions for  $\text{NH}_2\text{-SiC}$  nanosheets-modified electrodes (a) deposition potential (b) pH (c) deposition time

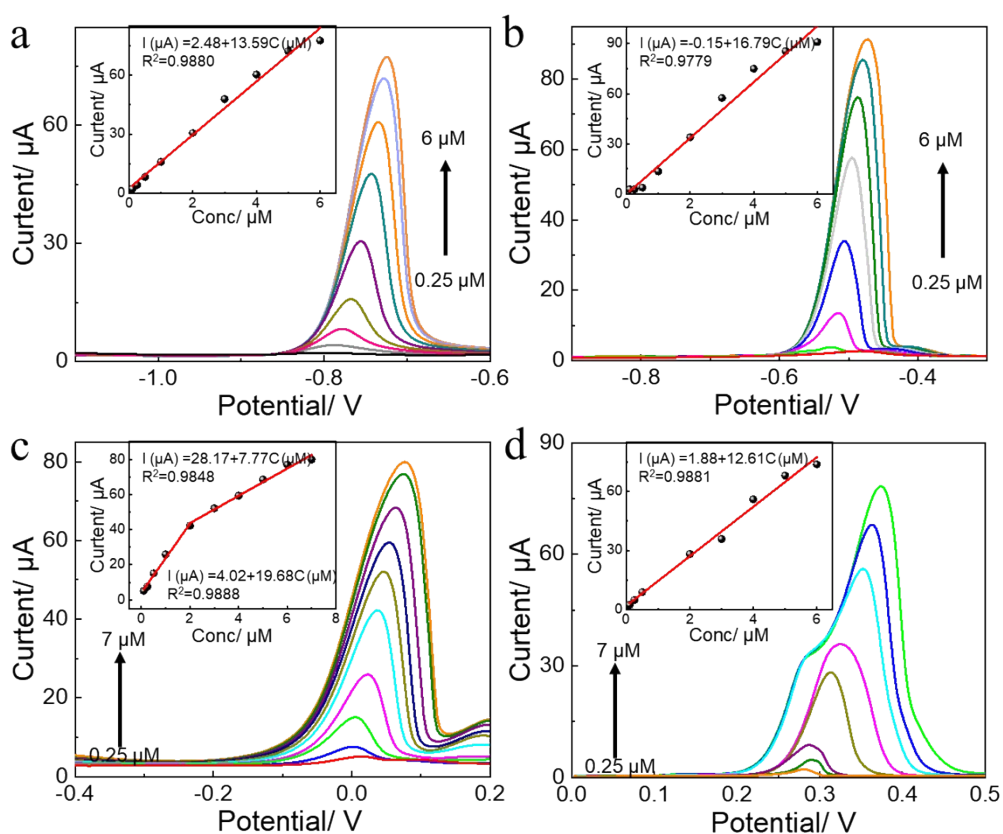


**Fig. S9** Individual detection of (a) $\text{Cd}^{2+}$ , (b) $\text{Pb}^{2+}$ , (c) $\text{Cu}^{2+}$  and (d) $\text{Hg}^{2+}$  using the  $\text{NH}_2\text{-SiC}$  nanowires-modified GCE. The upper-left insets show the corresponding curves of stripping peak current against HMIs concentration.

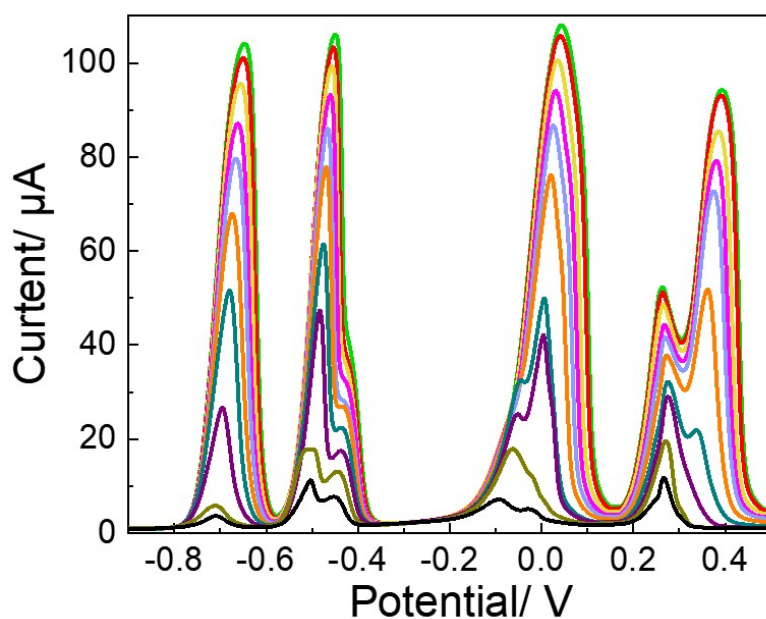


**Fig. S10** Simultaneous detection of  $\text{Cd}^{2+}$ ,  $\text{Pb}^{2+}$ ,  $\text{Cu}^{2+}$ , and  $\text{Hg}^{2+}$  using the  $\text{NH}_2\text{-SiC}$  nanosheets-modified GCE

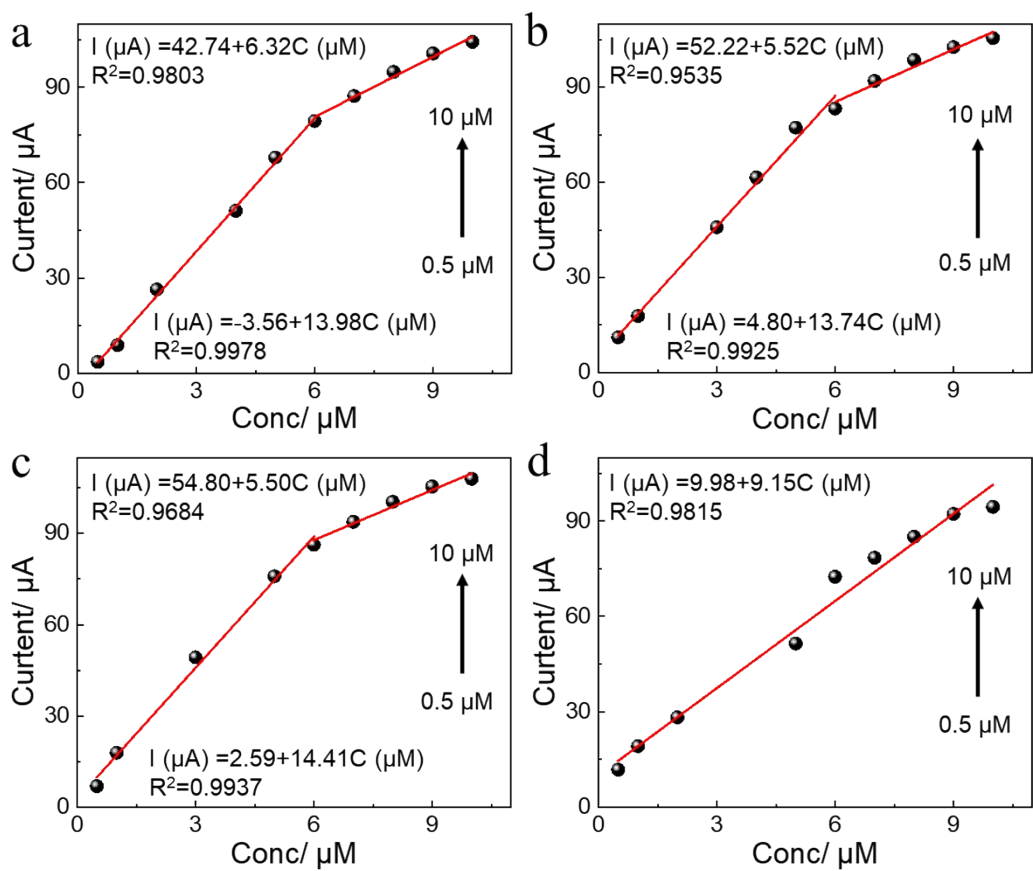


**Fig. S11** Calibration curves of SWASV stripping peak current against ion concentration for (a)  $\text{Cd}^{2+}$  (b)  $\text{Pb}^{2+}$  (c)  $\text{Cu}^{2+}$  (d)  $\text{Hg}^{2+}$  at  $\text{NH}_2\text{-SiC}$  nanowires-modified GCE